BIOCHEMISTRY

 Volume 45, Number 12 March 28, 2006

Accelerated Publications

High Yield of M-Side Electron Transfer in Mutants of *Rhodobacter capsulatus* Reaction Centers Lacking the L-Side Bacteriopheophytin†

Jessica I. Chuang,‡ Steven G. Boxer,‡ Dewey Holten,§ and Christine Kirmaier*,§

Department of Chemistry, Stanford University, Stanford, California 94305-5080, and Department of Chemistry, Washington University, St. Louis, Missouri 63130-4899

Received January 18, 2006; Revised Manuscript Received February 16, 2006

ABSTRACT: We present studies on a series of photosynthetic reaction center (RC) mutants created in the background of the *Rhodobacter capsulatus* D_{LL} mutant, in which the D helix of the M subunit has been substituted with that from the L subunit. Previous work on the D_{LL} mutant in chromatophore preparations showed that RCs assembled without the bacteriopheophytin H_L electron acceptor and performed no charge separation following light absorption. We have successfully isolated poly-His-tagged D_{LL} RCs by using the detergent Deriphat 160-C and shown that the RCs are devoid of H_L. The excited state of the primary electron donor, P*, is found to have a lifetime of 180 ± 20 ps and to decay exclusively (>95%) via internal conversion to the ground state, with no evidence for formation of any charge-separated intermediates. By additional mutation in the D_{LL} background of two residues that affect the P/P^+ oxidation potential and one that facilitates M-side electron transfer, we achieve an unprecedented 70% yield of $P^+H_M^-$, more than doubling the highest yield of this state achieved previously. This result underscores the importance of the relative free energies of P* and the charge-separated states in governing the rates and yields of electron transfer in bacterial RCs and provides a basis for systematically investigating M-side electron transfer without any competition from the native L-side pathway.

The three-dimensional structure of bacterial photosynthetic reaction centers (RCs)[1] transformed our understanding of the mechanism of light-driven electron transfer in photosynthesis. Among the most surprising revelations was the presence of two possible electron transfer pathways related by a local C_2 axis of symmetry, evident at the level of the reactive components as illustrated in Figure 1 (*1*). This structural symmetry is also maintained at the level of the secondary structures of the protein in the vicinity of the reactive components (the D helices of the L and M polypeptides are shown in Figure 1), but the symmetry is broken by differences in amino acids and more importantly at the level of function. In native RCs from several bacterial species, initial electron transfer proceeds with nearly 100% quantum efficiency and specificity along the reaction pathway shown

† This work was supported by a Hertz Graduate Fellowship to J.I.C. and the National Science Foundation (Grant MCB-0416623 to S.G.B. and Grant MCB-0314588 to D.H. and C.K.).

* To whom correspondence should be addressed. E-mail: kirmaier@wustl.edu. Phone: (314) 935-6480. Fax: (314) 935-4481.

‡ Stanford University.

§ Washington University.

[1] Abbreviations: RC, reaction center; BChl, bacteriochlorophyll; BPh, bacteriopheophytin; P, primary electron donor, a dimer of BChls; P_L, BChl macrocycle of P whose Mg is ligated by His L173; P_M, BChl macrocycle of P whose Mg is ligated by His M200; B_L and B_M, monomeric BChls on the L and M branches, respectively; H_L and H_M, L-branch and M-branch BPhs, respectively; Q_A and Q_B, primary and secondary quinone acceptors, respectively; LDAO, *N*-lauryl-*N*,*N*-dimethylamine *N*-oxide.

10.1021/bi0601048 CCC: $33.50
Published on Web 03/04/2006

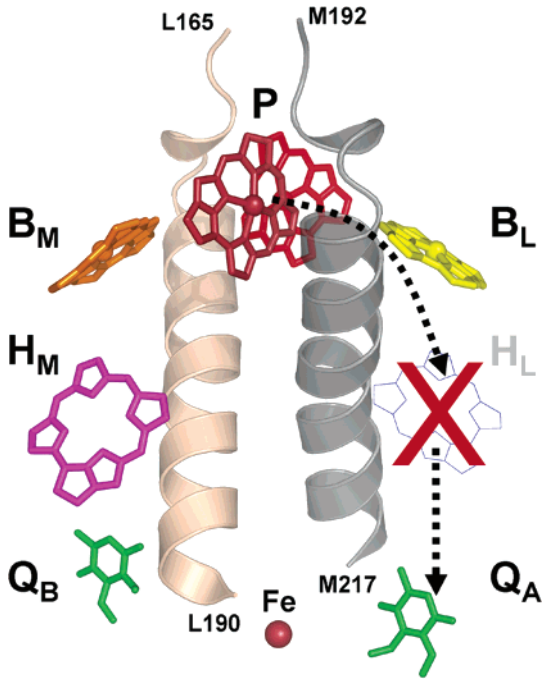

FIGURE 1: Arrangement of the wild-type L- and M-branch cofactors and the portion of the L polypeptide D helix (left) that is swapped into the M polypeptide D helix (right) in D_{LL}. H_L is missing from D_{LL} RCs [coordinates from PDB entry 1PCR (*1*)].

schematically at the right of Figure 1, denoted the L branch. This observation of unidirectional electron transfer led many labs to explore the basis of symmetry breaking by making individual amino acid replacements near the cofactors at symmetry-related sites that differ the most between the L branch and the nonfunctional M branch. Two residues of immediate focus were the Glu at position L104 (*2*) that hydrogen bonds to the bacteriopheophytin electron acceptor H_L (symmetry-related to Val at M131) and the Tyr at M208 (*3*−*6*) near bacteriochlorophyll B_L (symmetry related to Phe at L181). (References to M residues will use *Rhodobacter capsulatus* numbering throughout unless otherwise indicated.) Symmetrizing or changing these residues produced interesting, albeit relatively modest, effects on the primary electron transfer from P*, the excited state of the special pair, and no evidence for electron transfer along the M branch.

Two groups pursued much larger-scale symmetrization in *Rb. capsulatus*: the D_{LL} mutant (*7*, *8*), in which D helix residues M192−M217 that make contact with most of the reactive components were replaced with those at L165−L190 (Figure 1); and the *sym1* mutant (*9*), in which residues M187−M203 were replaced with L160−L176. Neither led to electron transfer to the M branch; however, both produced novel phenotypes. Remarkably, D_{LL} RCs assembled, but with H_L missing (Figure 1). In this case, the lifetime of P* was reported to be nearly 2 orders of magnitude longer than in wild type, consistent with the elimination of electron transfer along the L branch, but with no reported electron transfer to the M-branch pigments or evidence of charge separation to B_L. The long lifetime of P* made this a useful system for studying vibrational coherence in P* (*10*). Apparently, detergent-solubilized RCs were not stable as all studies were performed in chromatophore membranes, and no further analysis of chromophore composition, redox potentials, or electron transfer in this H_L-less mutant was reported. The *sym1* mutant led to the surprising discovery that P is much more difficult to oxidize to P^+ than in wild type. This was traced largely to the replacement of Phe at position M195 with His, which can hydrogen bond to the ring I acetyl group of the M macrocycle of P, P_M (*11*). Subsequently, residue M195, the symmetry-related residue at position L168, and those at positions L131 and M160 in *Rhodobacter sphaeroides* were all shown to systematically affect the oxidation potential of P, primarily by adding or removing hydrogen bonds to the acetyl or keto carbonyl groups of the two halves of P (*12*, *13*).

Recently, systematic efforts have led to the observation of M-branch electron transfer (reviewed in ref *14*). This began with a mutation, L(M212)H, which causes the assembly of RCs with a BChl (called β) in the H_L binding site (*15*). Since BChl is more difficult to reduce than BPh (by 150−300 meV in vitro), electron transfer to the L side was slowed. Using L(M212)H as a background, additional mutations were chosen by considering changes that would decrease or increase the free energies of charge-separated intermediates. One strategy was the insertion of a potentially positive or negative charge near B_M [S(L178)K] or B_L [G(M201)D] to favor or disfavor, respectively, the reduction of that cofactor (*16*, *17*). The most successful combination switched the Phe and Tyr residues at symmetry-related sites L181 and M208, respectively, following calculations suggesting that the tyrosine hydroxyl dipole stabilizes the B_L anion (and, by extension, would do the same for the B_M anion) (*18*−*20*). These mutations, combined with L(M212)H to form the YFH mutant in *Rb. capsulatus*, gave a 30% yield of $P^+H_M^-$, the highest yet observed (*21*). The remainder of P* decayed to give $P^+\beta^-$ or the ground state. Further increasing the M-branch yield clearly would be facilitated by the total prevention of L-branch electron transfer.

This is precisely the case in D_{LL} since H_L is absent, yet no evidence for electron transfer along the M branch or L branch (i.e., formation of $P^+B_L^-$) was reported. Our hypothesis was that this lack of activity, which we confirm below, can be understood in terms of the mutations in D_{LL} such as F(M195)H that increase the P/P^+ potential, disfavoring all the charge-separated states involving P^+. D_{LL} additionally contains the Y(M208)F mutation that also has been shown to destabilize $P^+B_L^-$ by removing a favorable interaction with B_L. On the basis of our cumulative understanding of the forces that control RC activity, the combination of D_{LL} plus mutations to restore the P/P^+ potential to nearer the wild-type value and the F(L181)Y mutation that stabilizes $P^+B_M^-$ should create more favorable conditions for charge separation to the M branch.

MATERIALS AND METHODS

Construction of His-Tagged D_{LL} Reaction Center Mutants. The plasmid pU2924 containing the D_{LL} mutation was isolated from *Rb. capsulatus* U43 cells by alkaline lysis (Mini-Prep Kit, Qiagen) and transformed into DH5α cells to obtain quantities sufficient for cloning. The 0.7 kb AscI−NcoI fragment of pU2924 containing the D_{LL} mutation was ligated into an M-gene shuttle vector, subcloned into the expression vector pUHTMluBgl:α-, and conjugated to host strain U43 as described previously (*22*). Note that because D_{LL} was reconstructed from the strain in Robles et al. (*8*),

Table 1: Regions of the *Rb. capsulatus* L and M Polypeptides that Are Modified in D_{LL} and Its Descendants (changes indicated in bold)

	M																										L	
	192	193	194	195	196	197	198	199	200	201	202	203	204	205	206	207	208	209	210	211	212	213	214	215	216	217	168	181
wild type	G	N	L	F	Y	N	P	F	H	G	L	S	I	A	A	L	Y	G	S	A	L	L	F	A	M	H	H	F
D_{LL}			L[a]	**H**						**M**		**G**		**S**	**L**	**F**	**F**	**T**	**T**		**W**	**A**	**L**					
D_{LL}-F_M										**M**		**G**		**S**	**L**	**F**	**F**	**T**	**T**		**W**	**A**	**L**					
D_{LL}-Y_LF_M										**M**		**G**		**S**	**L**	**F**	**F**	**T**	**T**		**W**	**A**	**L**					**Y**
D_{LL}-FY_LF_M										**M**		**G**		**S**	**L**	**F**	**F**	**T**	**T**		**W**	**A**	**L**				**F**	**Y**

[a] See Materials and Methods for details regarding the retention of Leu rather than Phe at this position.

M194 is a Leu rather than a Phe. This and all subsequent changes and their associated shorthand notation are summarized in Table 1. Site-directed mutagenesis was performed on L and D_{LL} M shuttle vectors using the QuikChange mutagenesis kit (Stratagene). The L and/or M genes were subcloned and conjugated as described above to yield the mutants D_{LL}-F_M [D_{LL} with H(M195)F], D_{LL}-Y_LF_M [D_{LL} with H(M195)F and F(L181)Y], and D_{LL}-FY_LF_M [D_{LL} with H(M195)F, H(L168)F, and F(L181)Y] (Table 1).

Reaction Center Growth and Purification. Bacterial growth and RC purification were performed as described by Laible et al. (*22*), except that following Ni affinity purification an anion exchange chromatography step was performed (Q Sepharose HP HiTrap, GE Healthcare). Final buffer conditions for all RCs were 10 mM Tris (pH 8) and 0.05% Deriphat 160-C unless otherwise noted.

Analysis of D_{LL} Pigment Composition. Low-temperature (77 K) absorption spectra of chromatophores and detergent-isolated RCs in 50% (v/v) glycerol were recorded in a liquid nitrogen cryostat. Pigment content was determined by three repetitions of acetone/methanol (7:2) solvent extraction under low-light conditions as described by van der Rest and Gingras (*23*).

Spectrochemical Measurement of P/P^+ Oxidation Potentials. The redox state of P was monitored by absorbance at 850 nm, and the potential was increased or decreased by addition of aliquots of ferricyanide or ascorbate, respectively. The potential was measured using a homemade Ag/AgCl electrode that was calibrated before each use with ferricyanide/ferrocyanide solutions. Measurements were corrected for Ag/AgCl versus NHE (220 mV).

Picosecond Transient Absorption Spectroscopy. The transient absorption measurements utilized 130 fs excitation and white-light probe flashes at 10 Hz. RCs (2.5−3 mL, 25−35 μM) were held in an ice-cooled reservoir and flowed through a 2 mm path length cell. This arrangement maintains a sample temperature of ~10 °C and ensures that fresh RCs are interrogated on each excitation flash. Further details can be found elsewhere (*21*).

RESULTS AND DISCUSSION

Characterization of His-Tagged, Detergent-Isolated D_{LL} Reaction Centers. The combination of Deriphat and the His tag makes possible the gentle and rapid isolation of D_{LL} RCs. Although the yield is low compared to that of wild type, once isolated, the RCs appear to be as stable as wild type. The 77 K absorption spectra of wild-type and D_{LL} His-tagged, detergent-isolated RCs are compared in Figure 2A. In D_{LL}, there is a decrease in the absorbance at 755 nm, and the band at 545 nm is no longer present, consistent with the absence of H_L. Pigment extraction yielded BChl:BPh ratios

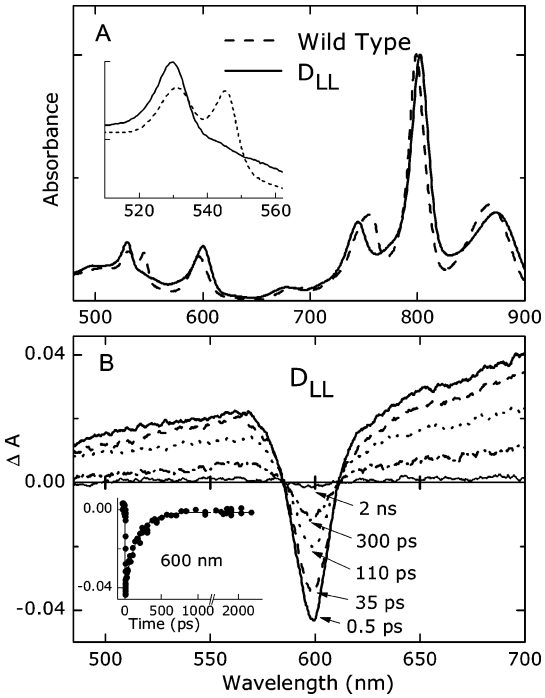

FIGURE 2: (A) Comparison of the 77 K absorption spectra of wild-type and D_{LL} His-tagged RCs in Deriphat/Tris buffer. (B) Transient absorption spectra acquired using 130 fs 850 nm excitation flashes (main). The inset shows the decay of the Q_X bleaching of P averaged between 593 and 605 nm (●) and a fit (—) to the instrument function plus one exponential (P* lifetime) plus a constant.

of 1.8 ± 0.2 for wild type and 4.1 ± 0.1 for D_{LL}, consistent with four BChls and two BPhs in wild type and four BChls and one BPh in D_{LL}. Also, the room-temperature and 77 K absorption spectra of chromatophores containing D_{LL} either with or without the His tag (not shown) are similar. We therefore conclude that the Deriphat-isolated, His-tagged D_{LL} RCs (1) lack any detectable pigment occupation of the H_L binding site and (2) are phenotypically similar to previously studied D_{LL} reaction centers in chromatophores.

Excitation of D_{LL} RCs with 850 nm 130 fs flashes produces the excited singlet state of the dimer, P*, which decays fully to the ground state (within a few percent) with a time constant of 180 ± 20 ps. Visible-region spectral and kinetic data are shown in Figure 2B. The P* difference spectrum acquired at 0.5 ps is identical to that obtained for P* in wild type and a host of other mutants, with a featureless singlet excited-state absorption throughout the 500−700 nm region broken by bleaching of the Q_X band of P at 600 nm. Bleaching of the Q_Y absorption band of P at 855 nm and stimulated emission at wavelengths to the red (extending to ~1000 nm) similarly accompany P* formation and decay fully to $\Delta A = 0$, reproducing the data reported previously in this spectral region for D_{LL} chromatophores. The visible-

region data (Figure 2B) are new and notably confirm that P* decays to the ground state in D_{LL} with no indication of formation of any charge-separated product. For D_{LL} RCs with the detergent exchanged to LDAO, the results are similar, but here P* has a shorter lifetime of 110 ± 10 ps.

Chemical redox titrations show that P in D_{LL} is at most 10% oxidized even in the presence of saturating concentrations of ferricyanide, indicating a P/P^+ potential that is ≥100 meV higher than in wild type. If other things are equal, this will increase the free energy of $P^+B_L^-$, $P^+B_M^-$, and $P^+H_M^-$ by ≥100 meV compared to that of wild type, as indicated in panels A and B of Figure 3. This simplistic view may reasonably hold for the two M-branch charge-separated states since there are no amino acid changes in D_{LL} near B_M or H_M. Therefore, $P^+B_M^-$ is likely even further in free energy above P* than it is in wild type, and $P^+H_M^-$ may be raised above P*. If $P^+H_M^-$ remains below P*, a time constant of >5 ns for its formation (using B_M as a superexchange mediator) would be noncompetitive with P* → ground-state deactivation and thus consistent with the data. On the L side, there are many changes near B_L, one of which, Y(M208)F, is known to destabilize $P^+B_L^-$. The specific effect on B_L^- is calculated to be ∼140 meV (*19*, *20*) and would add to the ≥100 meV higher P/P^+ oxidation potential, placing $P^+B_L^-$ well above P*. Of course, other residue changes may either counteract or add. The most simple interpretation of the lack of spectral or kinetic evidence for formation of $P^+B_L^-$ in D_{LL} is that this state is higher in free energy than P*, consistent with these first-order arguments.

Mutations in the D_{LL} Background that Favor M-Side Electron Transfer. To begin exploring how to reactivate D_{LL} for electron transfer, we restored M195 to the wild-type Phe in the D_{LL}-F_M mutant and in D_{LL}-Y_LF_M added F(L181)Y to foster electron transfer to the M side. Although the isolated RC yields are lower for both mutants than for D_{LL}, the RCs are stable in Tris/Deriphat, and low-temperature absorption spectra show the absence of H_L as in the original D_{LL} construct. Chemical redox titrations show that the P/P^+ potential in both mutants is ∼100 mV higher than the wild-type value. Y(M208)F is known to increase the oxidation potential of P by ∼30 meV (*4*, *5*). This may partially account for the fact that changing His M195 to Phe in the D_{LL} background is not sufficient to restore the wild-type potential (along with effects of other residue changes in D_{LL}). In D_{LL}-Y_LF_M, the F(L181)Y and Y(M208)F mutations should nearly balance each other with respect to their effects on the P/P^+ potential [shown previously for the F(L181)Y/Y(M208)F mutant (*5*)], again pointing to other changes that are part of the helix swap that affect the oxidation potential of P. Despite the high P/P^+ potential, both mutants give rise to some M-branch electron transfer. For both, the transient absorption spectrum acquired following P* decay shows bleaching at 527 nm and an anion band near 640 nm that are diagnostic of $P^+H_M^-$ formation. Preliminary analysis indicates that the yields of this state are a few percent in D_{LL}-F_M and ≤25% in D_{LL}-Y_LF_M, and that the remaining majority fraction of P* in both mutants decays to the ground state (data not shown). The strategy of lowering the P/P^+ potential and replacing Phe with Tyr at L181 to favor charge separation to the M branch clearly had the intended effect. Further details and analysis of these two mutants will be reported elsewhere.

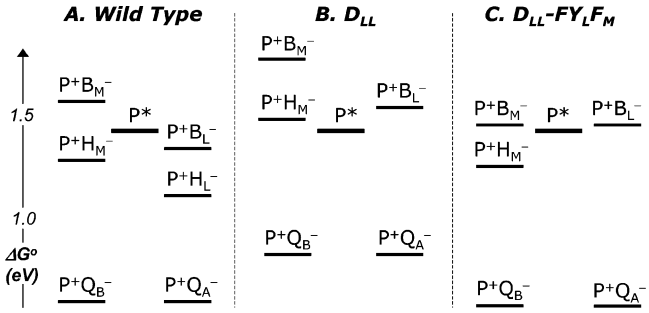

FIGURE 3: Working models proposed for the relative free energies of the charge-separated states in RCs from (A) wild type, (B) D_{LL}, and (C) D_{LL}-FY_LF_M.

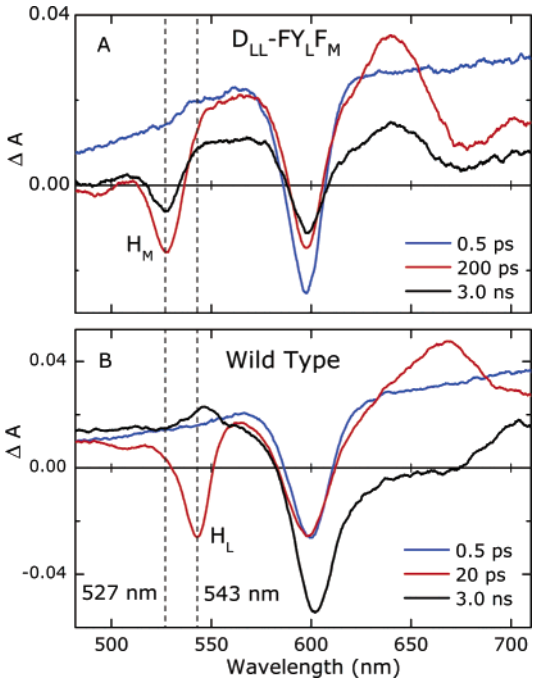

FIGURE 4: Comparison of the Q_X and anion region transient absorption spectra for D_{LL}-FY_LF_M (A) and wild type (B). Spectra were acquired using 130 fs flashes at 850 nm and are normalized to the same initial P* concentration for calculation of the yield of $P^+H_M^-$ in D_{LL}-FY_LF_M. See the text for further details.

To achieve our original goal of restoring the P/P^+ potential to near that of wild type, we added to D_{LL}-Y_LF_M the H(L168)F mutation, giving D_{LL}-FY_LF_M. This choice was guided by previous work that showed that removing the (native) hydrogen bond between L168 His and the ring I acetyl group of the L macrocycle of P decreases the P/P^+ potential by 80 mV in *Rb. sphaeroides* (*12*, *13*). Redox titrations show that D_{LL}-FY_LF_M has a P/P^+ potential ∼30 mV below that of wild type (475 ± 10 vs 505 ± 10 mV), and the ground-state absorption spectrum again is consistent with the loss of H_L (data not shown). A working model for D_{LL}-FY_LF_M is shown in Figure 3C. Sub-picosecond transient absorption data are shown in Figures 4−6. In summary, the data reveal that the P* lifetime in D_{LL}-FY_LF_M is ∼55 ps and that P* decays largely via M-branch electron transfer to give $P^+H_M^-$ in 70 ± 5% yield, with ground-state recovery accounting for the remaining 30% of P* decay.

The 70% yield of $P^+H_M^-$ is determined from the data in Figure 4. The P* spectrum acquired 0.5 ps after excitation (Figure 4A) is the same as that for D_{LL} (Figure 2) and wild-type RCs (Figure 4B). Analysis of the kinetics of the

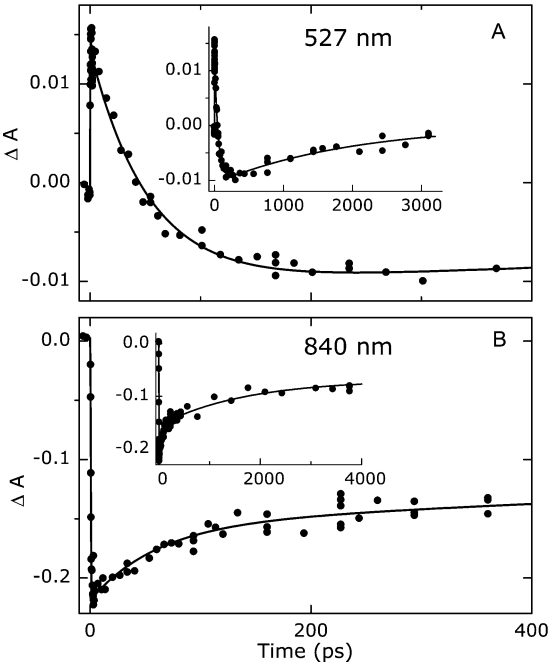

FIGURE 5: (A) Time course of the appearance and decay of the Q_X bleaching of H_M averaged between 523 and 531 nm (●) for D_{LL}-FY_LF_M following 130 fs excitation flashes at 850 nm. The solid line is a fit to the instrument response plus two exponentials (P* and $P^+H_M^-$ lifetimes) plus a constant, with one exponential fixed at 2 ns (for the $P^+H_M^-$ lifetime). (B) Decay of the Q_Y bleaching of P averaged between 835 and 845 nm (●) for D_{LL}-FY_LF_M following 130 fs excitation flashes at 590 nm. Fitting parameters are like those in panel A; see the text for further details.

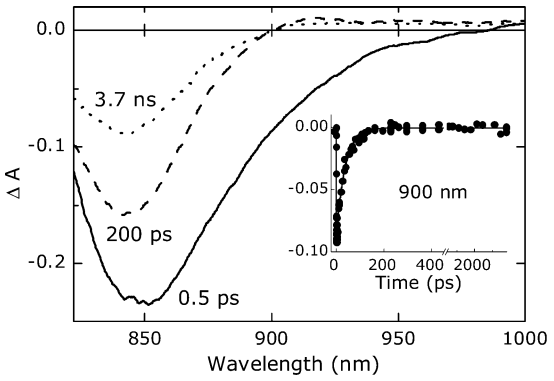

FIGURE 6: Transient absorption difference spectra for D_{LL}-FY_LF_M in the P bleaching region acquired at the times indicated following a 130 fs, 590 nm excitation flash. The inset shows the decay of the stimulated emission averaged between 895 and 905 nm (●) and a fit to the instrument function plus one exponential (P* lifetime) plus a constant (—).

appearance of the bleaching at 527 nm (presented below) gives a P* lifetime of 53 ± 10 ps. The spectrum acquired following P* decay at 200 ps is assigned to $P^+H_M^-$. It displays P bleaching near 600 nm, a large bleaching at 527 nm, and a smaller one at 495 nm that we assign to bleaching of the $Q_X(0,0)$ and $Q_X(1,0)$ bands of H_M, respectively, and a transient absorption with apparent peak at ∼640 nm that is assigned to the H_M anion. Analogous but red-shifted features of $P^+H_L^-$ are seen in the 20 ps spectrum of wild-type RCs (Figure 4B) with bleaching of the $Q_X(0,0)$ and $Q_X(1,0)$ bands of H_L at 543 and ∼505 nm, respectively, and the H_L anion band at 665 nm. The yield of $P^+H_M^-$ is calculated by normalizing the $P^+H_L^-$ and $P^+H_M^-$ spectra acquired at times corresponding to an equivalent number of P* lifetimes to the initial concentration of P* (via the magnitude of P bleach at ∼600 nm) and comparing the amplitudes of the H_M bleach of the mutant to the H_L bleach in wild type, and making the assumption that the H_L and H_M extinction coefficients are the same. By this analysis, $P^+H_M^-$ is formed in D_{LL}-FY_LF_M with a 70 ± 5% yield, more than doubling the highest previously reported yield of this state (30%), found in the YFH mutant of *Rb. capsulatus* (*21*). The reduction of bleaching of the Q_X band of P at ∼600 nm between 0.5 and 200 ps seen in Figure 4A (compared to no change for wild type in Figure 4B) indicates that decay of P* to the ground state accounts for the remaining 30% fraction of P*. This is independently confirmed by the data in the Q_Y band of P presented below.

Figure 5A shows kinetic data in the Q_X band of H_M and a fit to the instrument response plus two exponentials plus a constant. The time course of the appearance of the 527 nm bleaching reflects the P* lifetime; fits of the data between 515 and 540 nm return a value of 53 ± 10 ps. The decay of the 527 nm bleaching and, similarly, the decay of the 640 nm anion band give the lifetime of $P^+H_M^-$. This state has an ∼2 ns lifetime in YFH RCs in Tris/Deriphat and decays partially (∼60%) to the ground state and partially (∼40%) via electron transfer to Q_B (see ref *24* and unpublished results of H.-L. Kee, P. D. Laible, J. A. Bautista, D. K. Hanson, D. Holten, and C. Kirmaier). We expect a similar lifetime for $P^+H_M^-$ in D_{LL}-FY_LF_M, but the value can only be estimated from the experiments reported here because 4 ns is the longest time point acquired. A value of ∼1.5 ns is determined from fits to the decay of the 527 nm bleaching or from the decay of the 640 nm anion band, when this component is a free parameter. Essentially equally good fits are obtained with this value fixed at 2 ns. The 3.0 ns spectrum in Figure 4A clearly shows the same features as the 200 ps spectrum, but reduced in magnitude, consistent with only partial decay of $P^+H_M^-$. In wild-type RCs, $P^+H_L^-$ decays quantitatively with a 200 ps time constant to $P^+Q_A^-$ (3.0 ns spectrum in Figure 4B).

Analysis of the transient absorption spectra that probe the Q_Y absorption band of P gives similar results; relevant data are shown in Figures 5B and 6. The 0.5 ps spectrum of P* (Figure 6) displays P bleaching at ∼850 nm and stimulated emission (manifest as a negative Δ*A*) on the red side of the bleaching and extending past 950 nm. At wavelengths where only stimulated emission contributes (≥900 nm), the decay kinetics are described well by a single exponential. P* lifetimes ranging from 30 to 45 ps are determined between 900 and 930 nm; representative data are shown in the inset of Figure 6. At wavelengths where bleaching of P absorption contributes (830−900 nm), two exponentials are required to fit the kinetics, as clearly seen from the 840 nm data and fit in Figure 5B. One exponential gives the P* lifetime and the second the lifetime of $P^+H_M^-$ (∼2 ns, but again not rigorously determined in these experiments). The latter component will be manifest in the P bleaching decay because, as described above, we expect ∼60% of $P^+H_M^-$ to decay via ground-state recovery. For the P* lifetime, there is a smooth trend from longer values (70−80 ps) on the blue edge of P bleaching to shorter values (40−50 ps) approaching 900 nm as stimulated emission becomes more dominant. Detection wavelength-dependent or otherwise heterogeneous

P* lifetimes are not uncommon with a variety of origins posited (*25*). We take 55 ps as the P* lifetime determined in these experiments, which reflects the mean of the measurements in the Q_X and Q_Y absorption bands of P and P* stimulated emission.

The data averaged over the 835−845 nm interval and biexponential fit shown in Figure 5B also provide an independent measure of the relative yields of charge separation and ground-state recovery. Since the contribution of stimulated emission is expected to be insignificant at these wavelengths, the amplitudes of the two kinetic components both directly reflect ground-state recovery. The amplitude of the 55 ps P* decay component is ∼30% of the initial P-bleaching amplitude, which thus is a direct measure of the fraction of initial P* → ground state, with a 70% yield of charge-separated product(s) accounting for the bleaching remaining. These relative yields can also be seen by comparing the 0.5 and 200 ps spectra in Figure 6. These data are an independent measure of the yield of $P^+H_M^-$ determined from the changes in the P bleaching magnitude, under the assumption that this is the *only* charge-separated product. Clearly, both the kinetic and spectral data in the Q_Y band of P corroborate the 70% yield of $P^+H_M^-$ obtained from analysis of the data in the Q_X region.

The 55 ps P* lifetime and the 30% yield of ground-state recovery in D_{LL}-FY_LF_M determine a rate constant for internal conversion of P* to the ground state of 0.3/(55 ps) = $(183\ ps)^{-1}$. The same value (∼180 ps) is found for the P* lifetime in D_{LL} in Deriphat. Although the differences in the mutations near P in D_{LL} and D_{LL}-FY_LF_M in principle could affect the intrinsic P* lifetime, the agreement of these values supports the conclusion that P* deactivation to the ground state is the only means of P* decay in D_{LL}, dominating over any charge separation process. It is also noteworthy that the 110 ps intrinsic P* lifetime of D_{LL} in LDAO determined here is consistent with 80 and 110 ps values determined from the YF [F(L181)Y/Y(M208)F] and YFH mutants, respectively, also in LDAO (*21*, *26*). The differences found between the two detergents may be due in part to effects on the electronic structure of P, since the charge asymmetry in P* is known to affect its intrinsic lifetime (*27*). A longer intrinsic P* lifetime in Deriphat (or membranes) compared to LDAO would afford higher yields of charge separation (to either the L or M side). The 55 ps P* lifetime and 70% yield of $P^+H_M^-$ in the D_{LL}-FY_LF_M mutant determine a rate constant for (presumably) superexchange-mediated electron transfer from P* to the M side of 0.7/(55 ps) = $(78\ ps)^{-1}$. This value is similar to those of $(37\ ps)^{-1}$ and $(53\ ps)^{-1}$ found previously for the YFH and YF mutants in LDAO. Although there are obvious differences among YFH, YF, and D_{LL}-FY_LF_M, the consistency of the results underscores the important role of the F(L181)Y/Y(M208)F swap that is common to these three RCs.

Summary and Concluding Remarks. With only three changes in the D_{LL} construct, one reversion to a wild-type residue [H(M195)F] and two additional mutations [H(L168)F and F(L181)Y], D_{LL} has been transformed from a "dead" RC into D_{LL}-FY_LF_M, giving a 70% yield of M-branch electron transfer to H_M. The rationale for the changes was (1) to restore the P/P^+ oxidation potential to near that of wild type [H(M195)F and H(L168)F] and (2) to promote electron transfer to the M branch [F(L181)Y]. In D_{LL}-FY_LF_M, 11 changes remain in the substituted M polypeptide D helix in the vicinity of P, B_L, and the H_L-less site. A subset of these must be responsible for the absence of H_L; Watson et al. have recently reported that a single mutation results in an H_M-less RC (*28*). We are continuing to explore the individual and combined mutational effects of the D_{LL} helix swap on RC functionality and structure, including efforts to trap $P^+B_L^-$ and $P^+B_M^-$ and obtain more direct information about the energetics of these states.

ACKNOWLEDGMENT

We thank D. K. Hanson and P. D. Laible for the gift of wild-type cloning and expression vectors from ref *22* and P. Kanchanawong for acquisition of the low-temperature absorption spectra and assistance with mutagenesis.

REFERENCES

1. Ermler, U., Fritsch, G., Buchanan, S. K., and Michel, H. (1994) Structure of the Photosynthetic Reaction Centre from *Rhodobacter Sphaeroides* at 2.65 Å Resolution: Cofactors and Protein−Cofactor Interactions, *Structure 2*, 925−936.
2. Bylina, E. J., Kirmaier, C., McDowell, L. M., Holten, D., and Youvan, D. C. (1988) Influence of an Amino Acid Residue on the Optical Properties and Electron-Transfer Dynamics of a Photosynthetic Reaction Center Complex, *Nature 336*, 182−184.
3. Finkele, U., Lauterwasser, C., Zinth, W., Gray, K. A., and Oesterhelt, D. (1990) Role of Tyrosine M210 in the Initial Charge Separation of Reaction Centers of *Rb. sphaeroides*, *Biochemistry 29*, 8517−8521.
4. Nagarajan, V., Parson, W. W., Davis, D., and Schenck, C. C. (1993) Kinetics and Free Energy Gaps of Electron Transfer Reactions in *Rhodobacter sphaeroides* Reaction Centers, *Biochemistry 32*, 12324−12336.
5. Jia, Y., DiMagno, T. J., Chan, C.-K., Wang, Z., Du, M., Hanson, D. K., Schiffer, M., Norris, J. R., Fleming, G. R., and Popov, M. S. (1993) Primary Charge Separation in Mutant Reaction Centers of *Rhodobacter capsulatus*, *J. Phys. Chem. 97*, 13180−13191.
6. Laible, P. D., Greenfield, S. R., Wasielewski, M. R., Hanson, D. K., and Pearlstein, R. M. (1997) Antenna Excited-State Decay Kinetics Establish Primary Electron Transfer in Reaction Centers as Heterogeneous, *Biochemistry 36*, 8677−8685.
7. Breton, J., Martin, J. L., Lambry, J. C., Robles, S. J., and Youvan, D. C. (1990) Ground State and Femtosecond Transient Absorption Spectroscopy of a Mutant of *Rhodobacter capsulatus* which Lacks the Initial Electron Acceptor Bacteriopheophyrin, in *Structure and Function of Bacterial Photosynthetic Reaction Centers* (Michel-Beyerle, M. E., Ed.) pp 293−302, Springer-Verlag, New York.
8. Robles, S. J., Breton, J., and Youvan, D. C. (1990) Partial Symmetrization of the Photosynthetic Reaction Center, *Science 248*, 1402−1405.
9. Taguchi, A. K., Stocker, J. W., Alden, R. G., Causgrove, T. P., Peloquin, J. M., Boxer, S. G., and Woodbury, N. W. (1992) Biochemical Characterization and Electron-Transfer Reactions of sym1, a *Rhodobacter capsulatus* Reaction Center Symmetry Mutant Which Affects the Initial Electron Donor, *Biochemistry 31*, 10345−10355.
10. Vos, M. H., Lambry, J. C., Robles, S. J., Youvan, D. C., Breton, J., and Martin, J. L. (1991) Direct Observation of Vibrational Coherence in Bacterial Reaction Centers using Femtosecond Absorption Spectroscopy, *Proc. Natl. Acad. Sci. U.S.A. 88*, 8885−8889.
11. Stocker, J. W., Taguchi, A. K. W., Murchison, H. A., Woodbury, N. W., and Boxer, S. G. (1992) Spectroscopic and Redox Properties of Sym1 and (M)F195H: *Rhodobacter capsulatus* Reaction Center Symmetry Mutants Which Affect the Initial Electron-Donor, *Biochemistry 31*, 10356−10362.
12. Murchison, H. A., Alden, R. G., Allen, J. P., Peloquin, J. M., Taguchi, A. K. W., Woodbury, N. W., and Williams, J. C. (1993) Mutations Designed to Modify the Environment of the Primary Electron Donor of the Reaction Center from *Rhodobacter sphaeroides*: Phenylalanine to Leucine at L167 and Histidine to Phenylalanine at L168, *Biochemistry 32*, 3498−3505.

13. Lin, X., Murchison, H. A., Nagarajan, V., Parson, W. W., Allen, J. P., and Williams, J. C. (1994) Specific Alteration of the Oxidation Potential of the Electron Donor in Reaction Centers from *Rhodobacter sphaeroides*, *Proc. Natl. Acad. Sci. U.S.A. 91*, 10265−10269.
14. Wakeham, M. C., and Jones, M. R. (2005) Rewiring Photosynthesis: Engineering Wrong-Way Electron Transfer in the Purple Bacterial Reaction Center, *Biochem. Soc. Trans. 133*, 851−857.
15. Kirmaier, C., Gaul, D., DeBey, R., Holten, D., and Schenck, C. C. (1991) Charge Separation in a Reaction Center Incorporating Bacteriochlorophyll in Place of Photoactive Bacteriopheophytin, *Science 251*, 922−927.
16. Heller, B. A., Holten, D., and Kirmaier, C. (1995) Control of Electron Transfer to the L-Side versus the M-side of the Photosynthetic Reaction Center, *Science 269*, 940−945.
17. Kirmaier, C., Weems, D., and Holten, D. (1999) M-side Electron Transfer in Reaction Center Mutants with a Lysine Near the Nonphotoactive B Bacteriochlorophyll, *Biochemistry 38*, 11516−11530.
18. Parson, W. W., Chu, Z. T., and Warshel, A. (1990) Electrostatic Control of Charge Separation in Bacterial Photosynthesis, *Biochim. Biophys. Acta 1017*, 251−272.
19. Alden, R. G., Parson, W. W., Chu, Z. T., and Warshel, A. (1996) Orientation of the OH Dipole of Tyrosine (M)210 and Its Effect on Electrostatic Energies in Photosynthetic Bacterial Reaction Centers, *J. Phys. Chem. 100*, 16761−16770.
20. Gunner, M. R., Nicholls, A., and Honig, B. (1996) Electrostatic Potentials in *Rhodopseudomonas viridis* Reaction Centers: Implications for the Driving Force and Directionality of Electron Transfer, *J. Phys. Chem. 100*, 4277−4291.
21. Kirmaier, C., He, C., and Holten, D. (2001) Manipulating the Direction of Electron Transfer in the Bacterial Reaction Center by Swapping Phe for Tyr Near $BChl_M$ (L181) and Tyr for Phe Near $BChl_L$ (M208), *Biochemistry 40*, 12132−12139.
22. Laible, P. D., Kirmaier, C., Udawatte, C. S. M., Hofman, S. J., Holten, D., and Hanson, D. K. (2003) Quinone Reduction via Secondary B-Branch Electron Transfer in Mutant Bacterial Reaction Centers, *Biochemistry 42*, 1718−1730.
23. Van der Rest, M., and Gingras, G. (1974) The Pigment Complement of the Photosynthetic Reaction Center Isolated from *Rhodospirillum rubrum*, *J. Biol. Chem. 249*, 6446−6453.
24. Kirmaier, C., Laible, P. D., Hanson, D. K., and Holten, D. (2003) B-side Charge Separation in Bacterial Photosynthetic Reaction Centers: Nanosecond-Timescale Electron Transfer from H_B^- to Q_B, *Biochemistry 42*, 2016−2024.
25. Woodbury, N. W., Peloquin, J. M., Alden, R. G., Lin, X., Lin, S., Taguchi, A. K. W., Williams, J. C., and Allen, J. P. (1994) Relationship between Thermodynamics and Mechanism during Photoinduced Charge Separation in Reaction Centers from *Rhodobacter sphaeroides*, *Biochemistry 33*, 8101−8112.
26. Kirmaier, C., Laible, P. D., Hanson, D. K., and Holten, D. (2004) B-side Electron Transfer to form P^+HB^- in Reaction Centers from the F(L181)Y/Y(M208)F Mutant of *Rhodobacter capsulatus*, *J. Phys. Chem. B 108*, 11827−11832.
27. Laporte, L. L., Palaniappan, V., Davis, D. G., Kirmaier, C., Schenck, C. C., Holten, D., and Bocian, D. F. (1996) Influence of Electronic Asymmetry on the Spectroscopic and Photodynamic Properties of the Primary Electron Donor in the Photosynthetic Reaction Center, *J. Phys. Chem. 100*, 17696−17707.
28. Watson, A. J., Fyfe, P. K., Frolov, D., Wakeham, M. C., Nabedryk, E., Van Grondelle, R., Breton, J., and Jones, M. R. (2005) Replacement or Exclusion of the B-Branch Bacteriopheophytin in the Purple Bacterial Reaction Centre: The H_B Cofactor is not Required for Assembly or Core Function of the *Rhodobacter sphaeroides* Complex, *Biochim. Biophys. Acta 1710*, 34−46.

BI0601048